International Journal of Thermal Sciences 49 (2010) 218–224

Contents lists available at ScienceDirect

International Journal of Thermal Sciences

journal homepage: www.elsevier.com/locate/ijts

Crosswinds effect on the performance of natural draft wet cooling towers

Rafat Al-Waked*

Mechanical Engineering Department, College of Engineering, Dhofar University, PO Box 2509, Salalah, Dhofar 211, Sultanate of Oman

ARTICLE INFO

Article history:
Received 24 February 2009
Received in revised form
5 June 2009
Accepted 10 July 2009
Available online 14 August 2009

Keywords:
Thermal performance
CFD
Multiphase flow
Cooling tower
Heat and mass transfer

ABSTRACT

Effects of crosswinds on the thermal performance of natural draft wet cooling towers (NDWCTs) have been investigated. A three-dimensional CFD model has been used to determine the effect of crosswinds on NDWCTs performance surrounded by power plant building structures. The three-dimensional CFD model has utilized the standard k–ε turbulence model as the turbulence closure. Two cases have been investigated: a stand-alone NDWCT and two NDWCTs within a proposed power plant structures (PPS). It has been found that regardless of the crosswinds direction, an increase of 1.3 k or more could be predicted at crosswinds speeds greater than 4 m/s. Furthermore, the performance of NDWCTs under crosswinds has been found to be dependent on the three major factors: the structure of the approaching crosswinds and whether it is disturbed or undisturbed, the location of the NDWCT in the wake of the other NDWCT, and the location of the NDWCT in front of/in the wake of the PPS. When comparing results from the stand-alone and from the NDWCTs within PPS simulations, differences in ΔT_{wo} were found to be less than 1 K for the whole span of crosswinds speeds and could be decreased to 0.7 K for speeds less than 8 m/s. Finally, results obtained from the simulation of a stand-alone NDWCT could be used instead of those from NDWCTs within PPS at a certain crosswinds direction for qualitative comparisons.

1. Introduction

In the design of natural draft wet cooling towers (NDWCTs), effect of crosswinds on their thermal performance is taken into account under the assumption that the NDWCT is an isolated structure. However, NDWCTs are often in close proximity to each other or to other buildings where wind-induced pressures can be significantly different from those on an isolated tower. Ignoring the group effect on NDWCTs during the design process has proven to underestimate their thermal performance.

A NDWCT, similar to the one shown in Fig. 1, is the cornerstone of the cooling system in use in large modern thermal power plants. In NDWCTs, a combination of heat and mass transfer effects are used to cool the water coming from the turbine's condenser. The hot water, coming from the condenser, is sprayed on top of splash bars or film fills in order to expose a very large portion of water surface to the cooling ambient air. The moisture content of the cooling air is less than the moisture content of the saturated air at the hot water temperature, which results in evaporating an amount of water. The energy required for evaporation is extracted from the remaining water, hence reducing its temperature. The cooled water is then collected at the basin of the NDWCT and is pumped back into the condenser completing its circuit.

As the heat of the water is transferred to the air passing through the tower, the warmed air rises and draws in fresh air at the base of the tower which makes the cooling process dependent on crosswinds conditions. Inefficiency in the cooling process of these towers results in a continuous loss of power generation. The degradation in thermal performance of cooling towers after installation has highlighted the importance of crosswinds.

Airflow around full-scale NDWCTs has Reynolds number (Re) of the order (10^8). However, previous comprehensive wind-tunnel experiments [12,13,18,19] on cylindrical bodies and NDWCTs were conducted at a subcritical Re ($Re \leq 3.9 \times 10^5$). These experiments did not take into consideration the effect of the coupled flow in- and out-of the tower because of difficulties and complexities in conducting such experiments. Therefore, different approaches need to be adopted to overcome these limitations.

On the thermal side of NDWCTs, most of the reported work focused on the description of both buoyant jets and plumes [3,9,10]. These studies have covered the simplest analytical models, higher-level integral models, numerical predictions using CFD and experimental studies. The main concentration of those studies, however, was on single plumes with fewer studies reported on multiple plumes [6,11]. One of the significant findings from the study of multiple plumes was the non-existence of symmetry in the flow at certain conditions.

* Tel.: +968 23225061x127; fax: +968 23225814.
E-mail address: rafat@unswalumni.com

1290-0729/$ – see front matter © 2009 Elsevier Masson SAS. All rights reserved.
doi:10.1016/j.ijthermalsci.2009.07.012

Nomenclature

C_D	Drag coefficient (–)
C_p	Specific heat (J kg^{-1} K^{-1})
d	Diameter (m)
D	Diffusion coefficient of vapour (m^2 s^{-1})
F	Momentum (N m)
h	Convective heat transfer coefficient (W m^{-2} K^{-1})
H_i	Height of the NDWCT inlet (m)
h_{fg}	Latent enthalpy of evaporation (kJ kg^{-1})
k	Turbulent kinetic energy (m^2 s^{-2})
k	Conductivity coefficient (W m^{-1} K^{-1})
M	Mass (kg)
m_f	Mass fraction (–)
m_p	Mass of a particle (kg)
$\dot{m}_p$	Mass flow rate of the particles (kg s^{-1})
Nu	Nusselt Number
Pr	Prandtl Number
Q	Heat transferred (W)
Re	Reynolds Number
Sc	Schmidt Number
Sh	Sherwood Number
T	Temperature (K)
t	Time (s)
V_p	The component of the flow velocity perpendicular to the surface (m s^{-1})
u, v, w	Velocity components in x-, y- and z-direction respectively (m s^{-1})
x, y, z	The Cartesian co-ordinates
y	Height above ground level (m)

Greek letters

ε	Turbulent kinetic energy dissipation rate (m^2 s^{-3})
ρ	Density (kg m^{-3})
Δ	Difference in temperature (K)

Subscripts

a	Air
cw	Crosswinds
D	Drag
ma	Moist air
p	Particle (water droplet)
ref	Reference point, considered to be at 10 m above ground level
v	Vapour
w	Water
0	Initial value

With the advancement in computer technology, CFD has become a vital analysis and research tool that can overcome most of the wind-tunnel limitations. Extensive work has been published focusing on the thermal performance of natural draft dry cooling towers (NDDCTs) [1,7,17]. However, work done on the thermal performance has considered an isolated NDDCT as the simulation model. Bender et al. [4,5] investigated the effect of crosswinds on a double-cell mechanical induced cooling tower. They examined the flow over a prototype mechanical induced cooling tower using a two-dimensional finite-volume numerical model. Currently, there is no published work available demonstrating numerically the effect of the interaction of NDWCTs, within a power plant, on their thermal performance.

In this paper, A three-dimensional CFD analysis has been conducted to investigate effects of crosswinds on the thermal performance of NDWCTs within a power plant.

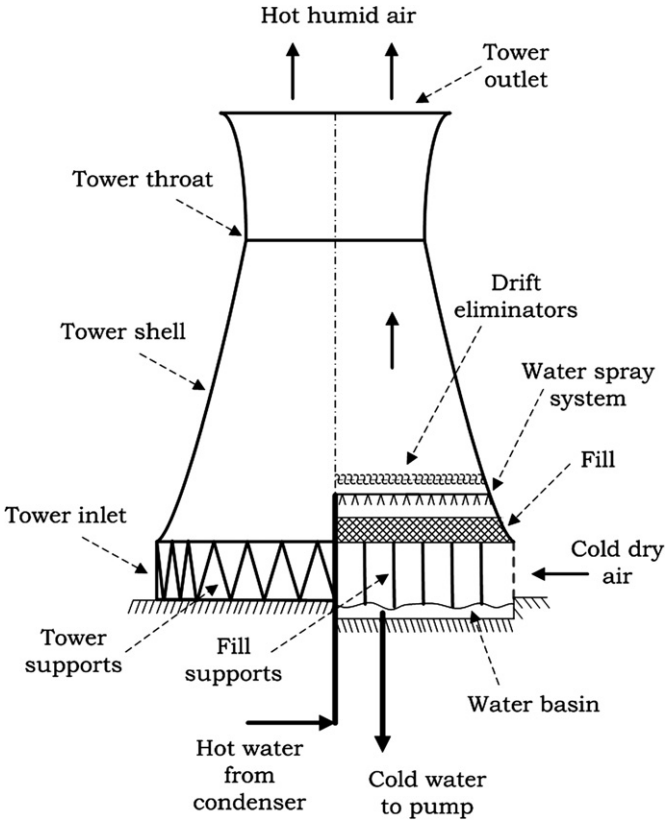

Fig. 1. Counter-flow natural draft wet cooling tower.

2. Governing equations

In FLUENT [8], the airflow is solved as a continuous phase using the steady state Eulerian approach while droplet trajectories are solved as a dispersed phase using the unsteady state Lagrangian approach. The airflow equations that describe heat, mass and

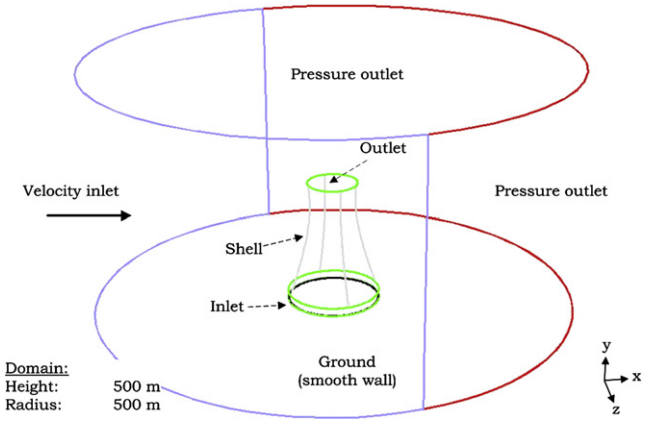

Fig. 2. General view of the stand-alone NDWCT and the utilized boundary conditions.

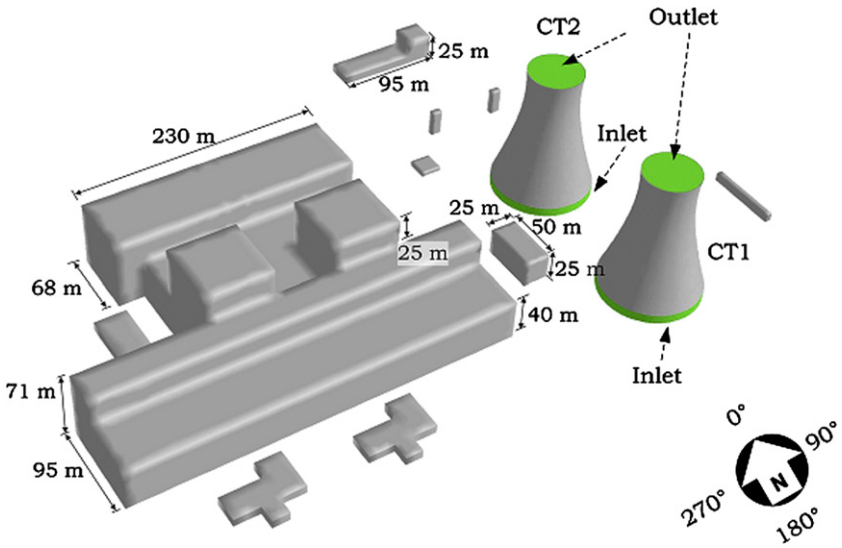

Fig. 3. General view of the NDWCTs within PPS and the adopted crosswinds directions.

momentum transfer can be written as a general equation having the form:

$$\nabla\cdot\left(\rho_{\mathrm{ma}}u\phi-\Gamma_{\phi}\nabla\phi\right)=S_{\phi}+S_{\mathrm{p}\phi} \tag{1}$$

where ρ_{ma} is the moist air density, u is the velocity vector, ϕ is the scalar quantity for u, v, w, T, Y_{v}, k and ε, Γ_{ϕ} is the diffusion coefficient, S_{ϕ} is the source term for the air phase and $S_{\mathrm{p}\phi}$ is the additional source due to the interaction between the air and the water droplets.

Heat transferred from the water droplet into the surrounding air inside the NDWCT consists of both convective and evaporative heat transfer. The heat transfer coefficient (h) is evaluated using the correlation of Ranz and Marshal [15,16] as defined in Eq. (2). Similarly, the mass transfer coefficient (h_{m}) is calculated from the Reynolds analogy based on the unity of Lewis number ($Sc_{\mathrm{ma}}/Pr_{\mathrm{ma}}=1.0$) as defined in Eq. (3) [8].

$$Nu=\frac{hd_{\mathrm{p}}}{k_{\mathrm{ma}}}=2.0+0.6Re^{0.5}Pr_{\mathrm{ma}}^{0.33} \tag{2}$$

$$Sh=\frac{h_{\mathrm{m}}d_{\mathrm{p}}}{D_{\mathrm{va}}}=2.0+0.6Re^{0.5}Sc_{\mathrm{ma}}^{0.33} \tag{3}$$

Heat, mass and momentum gained or lost by any stream of water droplets that follow the same trajectory to the surrounding air are calculated and are incorporated into the subsequent air phase calculation as source terms ($S_{\mathrm{p}\phi}$) according to Eq. (4–6) respectively.

$$Q=\left[\frac{M_{\mathrm{p,av}}}{M_{\mathrm{p,0}}}c_{\mathrm{p,p}}\Delta T_{\mathrm{p}}+\frac{\Delta M_{\mathrm{p}}}{M_{\mathrm{p,0}}}\left(-h_{\mathrm{fg}}+\int_{T_{\mathrm{ref}}}^{T_{\mathrm{p}}}c_{\mathrm{pv}}\mathrm{d}T\right)\right]\dot{m}_{\mathrm{p,0}} \tag{4}$$

$$M=\frac{\Delta M_{\mathrm{p}}}{M_{\mathrm{p,0}}}\dot{m}_{\mathrm{p,0}} \tag{5}$$

$$F=\sum\left(\frac{3}{4}\frac{\mu C_{\mathrm{D}}Re}{\rho_{\mathrm{p}}d_{\mathrm{p}}^{2}}(v_{\mathrm{p}}-v)\right)\dot{m}_{\mathrm{p,0}}\Delta t \tag{6}$$

The heat exchanged between the water droplet and the air, presented by Eq. (4), consists of two terms. The first term on the right hand side represents the sensible heat and the second term represents the latent heat transferred from/to the water droplet as it crosses the control volume (mesh element). The latent heat term is the result of the mass transfer from the droplet and it consists of the latent heat of vaporisation (h_{fg}) and species enthalpy (vapour).

3. Boundary conditions

A cylindrical numerical domain with a height and a radius of 500 m has been utilized to simulate the stand-alone NDWCT as shown in Fig. 2. The NDWCT under investigation is 129.8 m high with a base diameter of 95.2 m and an inlet height of 8.6 m. The numerical domain radius has been expanded to 1000 m to accommodate the power plant structures (PPS) shown in Fig. 3. The final numerical domain consists of 820 thousand structured and unstructured (hybrid) mesh elements. The number of mesh elements has been kept constant for all cases under investigation. In addition, the mesh element size has been smoothly stretched to resolve the high gradient regions and to ensure an accurate resolution of both temperature and velocity fields.

At the inlet of the CFD domain, a velocity boundary has been utilized where air dry-bulb temperature (T_{adb}) and vapour mass fraction (m_{fv}) have been provided in accordance with Table 1. In addition, crosswinds speed has been provided according to Eq. (7) in which the reference speed is evaluated at an elevation of 10 m above ground level [14].

$$\frac{U_{\mathrm{cw}}}{U_{\mathrm{cw,ref}}}=\left(\frac{y}{y_{\mathrm{ref}}}\right)^{0.2} \tag{7}$$

Table 1
Design conditions and dimensions of the NDWCT.

	Reference conditions
Air dry-bulb temperature (T_{adb})	297.1 K
Air wet-bulb temperature (T_{awb})	291.5 K
Atmospheric pressure (P_{atm})	91.0 kPa
Droplet diameter (D_{p})	5 mm
Number of nozzles	5097
Vapour mass fraction (m_{fv})	0.012
Water inlet temperature (T_{wi})	315.3 K

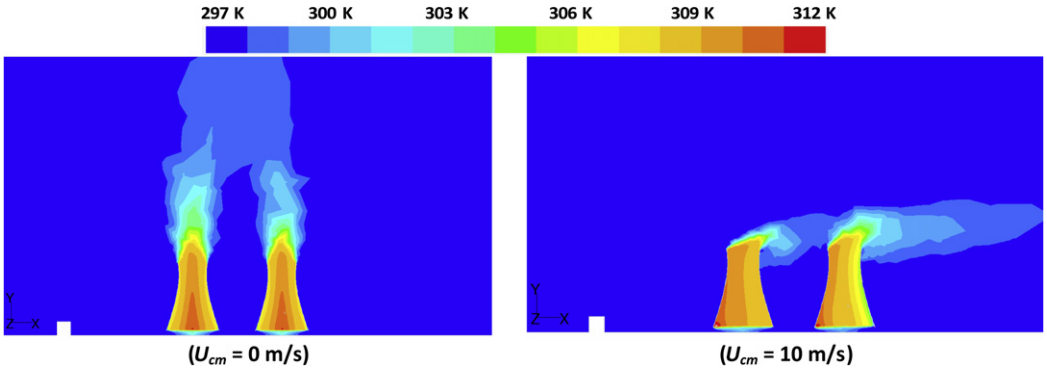

Fig. 4. Air temperature contours for NDWCTs within PPS at $\theta_{cw} = 0^{\circ}$.

At the pressure outlet boundary, both T_{adb} and m_{fv} have been given the same values as those at the velocity inlet boundary. Instead of providing the velocity magnitude, the gauge pressure with reference to the atmospheric pressure given in Table 1 has been provided. The wall boundary condition has been used to bound the fluid and solid regions. The no-slip boundary condition has been used at the solid boundaries, ground and NDWCT's shell.

When the water flows out of the spray nozzles, it forms a three-dimensional stream of water droplets. Initial velocity and direction of the stream have been provided at the beginning of the simulation, in addition to inlet water temperature, mass flow rate and droplet diameter. More details of the CFD model have been reported in earlier work of the author where the validation of the CFD code was made [2].

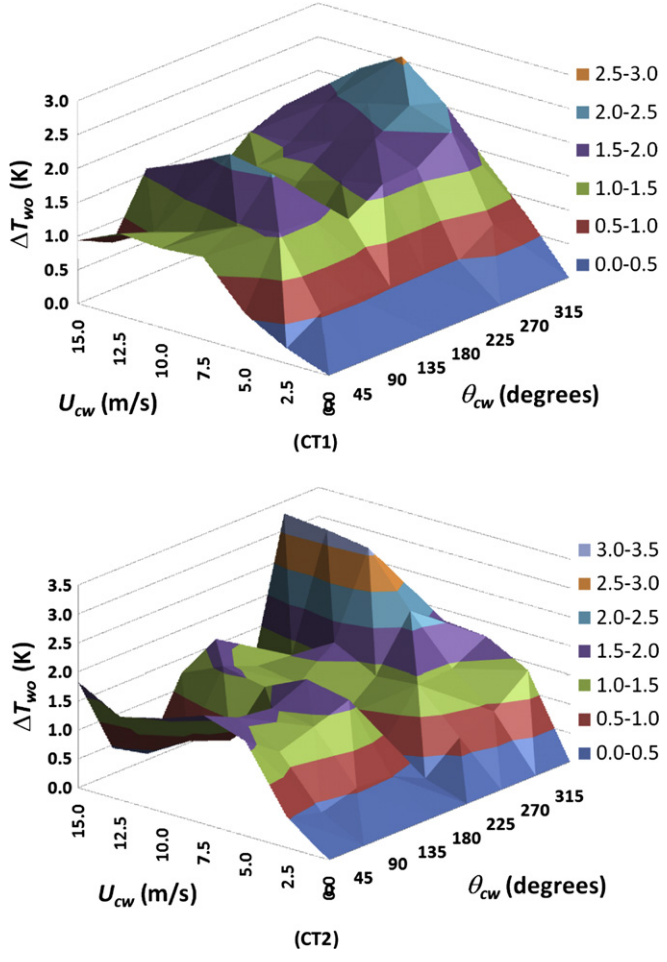

Fig. 5. Coloured contours showing ΔT_{wo} of the NDWCTs within PPS under crosswinds.

4. Results and discussion

Effects of crosswinds direction have been investigated by considering eight approaching angles ($\theta_{cw} = 0^{\circ}$, 45°, 90°, 135°, 180°, 225°, 270° and 315°) with crosswinds approaching from the North given a zero approach angle ($\theta_{cw} = 0^{\circ}$). Furthermore, at each crosswinds direction six crosswinds speeds have been investigated.

4.1. Crosswinds effects

In the absence of crosswinds ($U_{cw} = 0$ m/s), airflow nature within the NDWCT is a result of the upward natural current caused by the falling hot water droplets as shown by Fig. 4. As the air flows across the rain zone, it exchanges both heat and mass with hotter water droplets and loses momentum due to the drag effect. The deeper the air flows into the rain zone, the hotter, slower and more humid it gets. Consequently, the air at the centreline of the NDWCT has the highest temperature and humidity and the lowest velocity. As the crosswinds speed increases ($U_{cw} = 10$ m/s), the hot air spots start shifting toward the windward side of the tower as can be seen from [2] Fig. 4.

The existence of PPS adjacent to the NDWCTs has caused them to react differently to crosswinds speeds. Their thermal performances have been affected slightly at crosswinds speed of 2.5 m/s for all the simulated direction as shown in Fig. 5. The highest performance has been found when each of the NDWCTs is located in the wake of the other, i.e. at ($\theta_{cw} = 0^{\circ}$, 180°). The effect of PPS on the performance of the NDWCTs was not significant at this low speed. However, high crosswinds speeds have deteriorated the NDWCTs performances uniformly and caused the increase of ΔT_{wo} by 1.9 K at crosswinds speed of 5 m/s.

The performance of the NDWCT became more dependent on its location within the PPS as crosswinds speed increases. The location of CT1, as shown in Fig. 3, makes it exposed to undisturbed crosswinds over a wide range of crosswinds approaching angles ($\theta_{cw} = 135^{\circ}$, 180° and 225°) whereas, CT2 is exposed at $\theta_{cw} = 45^{\circ}$. At all the other θ_{cw}, CT1/CT2 is positioned in the wake of either CT2/CT1 or the PPS which has affected its performance. For CT2, the highest performance found ($\Delta T_{wo} < 0.5$ K) has occurred at crosswinds speeds of ($U_{cw} > 12$ m/s) and a direction of ($\theta_{cw} = 90^{\circ}$). The lowest performance found ($\Delta T_{wo} > 3$ K) has occurred at crosswinds speeds of ($U_{cw} > 12$ m/s) and a direction of ($\theta_{cw} = 270^{\circ}$). The performance of CT1, on the other hand, was the lowest ($\Delta T_{wo} > 2.5$ K) when it was located behind the PPS ($\theta_{cw} = 270^{\circ}$,

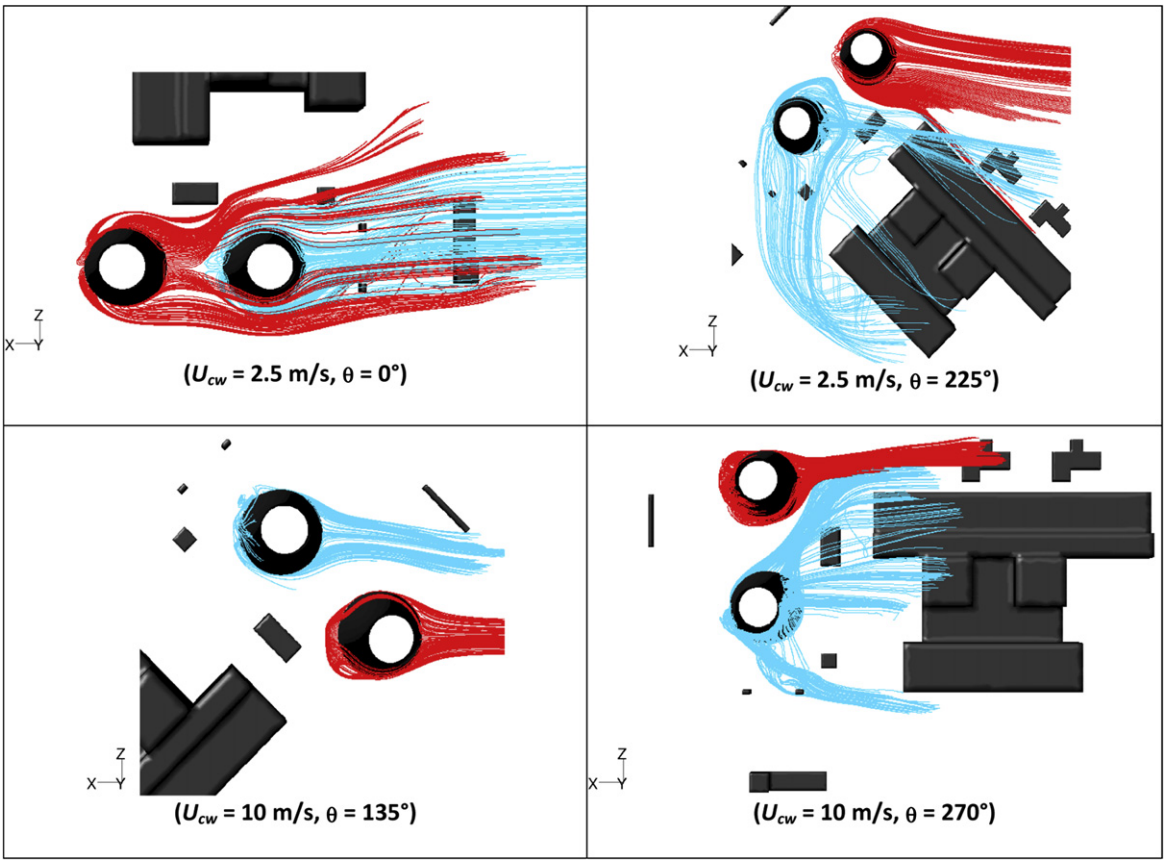

Fig. 6. Path lines showing the airflow structure around the NDWCTs within PPS at $U_{cw} = 2.5$ m/s. The lines are originated from the NDWCT inlet to show where the flow to the NDWCT inlet is coming from.

315°) at crosswinds speeds of ($8 < U_{cw} < 10$ m/s). At crosswinds direction of ($\theta_{cw} = 135°$) and speeds of ($10 < U_{cw} < 12.5$ m/s), CT1 has performed very well ($\Delta T_{wo} < 0.7$ K).

It is worth mentioning that the increase in water temperature as a function of crosswinds velocity in the current study is purely dependent on the assumption of an equal distribution of crosswinds velocity. This means that the crosswinds approach the NDWCTs from all directions and across the whole speed range are of equal weights. This is not true in real applications where crosswinds normally have relatively low speed around 4–8 m/s and approaches more frequently from certain directions. Therefore, a study of crosswinds history from the weather station at the power plant based on the result of the current study could demonstrate how severe crosswinds affect the performance of NDWCTs.

The reported variations in the performance of the NDWCTs were a result of the variation in airflow structures around them. The buoyancy forces within the NDWCTs, at no crosswinds condition, have induced the air to flow into the towers at an average speed of 4 m/s. At crosswinds speeds of less than 4 m/s, the two NDWCTs reacted similarly to the change in crosswinds direction. As it can be seen from Fig. 6, the NDWCTs extracted air mainly from the approaching crosswinds. The existence of PPS in the middle between the approaching crosswinds and the NDWCTs has not prevented the NDWCTs from extracting the air from high-level, top of the PPS, and from the both side of the PPS ($\theta_{cw} = 225°, 315°$). This applies also to the situation where one of the NDWCTs stands in the wake of the other NDWCT.

The general features of the flow structure remained the same at high crosswinds speeds compared to the flow structure at the speed of 2.5 m/s. However, two main differences in the flow structure were found. First, the airflow streams started approaching the NDWCT inlet in a thinner bundle across a small span angle. This is due to the availability of large amount of air at this high speed that can meet the draft requirements of the NDWCTs. Second, air flowing into the NDWCTs was limited to the crosswinds approaching angle especially when the NDWCTs were in the wake of the PPS ($\theta_{cw} = 225°, 315°$). Furthermore, it has been noticed that the NDWCT located in the wake of the other NDWCT performed slightly better than being in the wake of the PPS. The air flowing around the windward NDWCT has been redirected toward the inlet of the NDWCT at the back. This airflow recovery is dependent on the dimension of the NDWCT at the base.

The dimension of the NDWCT base is almost one-third of that of the PPS; hence, the wake behind the PPS is expected to be much larger than that behind the NDWCT. The wake behind the PPS has created a low-pressure zone that has reduced the amount of air flowing into the NDWCT. Consequently, the performance of the NDWCT has been found to be lower than that of the NDWCT in the wake of another NDWCT.

The differences in the performance of the NDWCTs due to the change in crosswinds conditions and the location within the PPS are shown in Fig. 7a. A positive value of ΔT means that CT2 is thermally performing better than CT1 under crosswinds and the opposite is true for a negative value of ΔT. A better/higher performance of the NDWCT means that crosswinds have not degraded its performance as bad as the other NDWCT within the proposed PPS. Differences in the range of ± 1.5 K have been found between the two NDWCTs of which around 40% of the simulated crosswinds

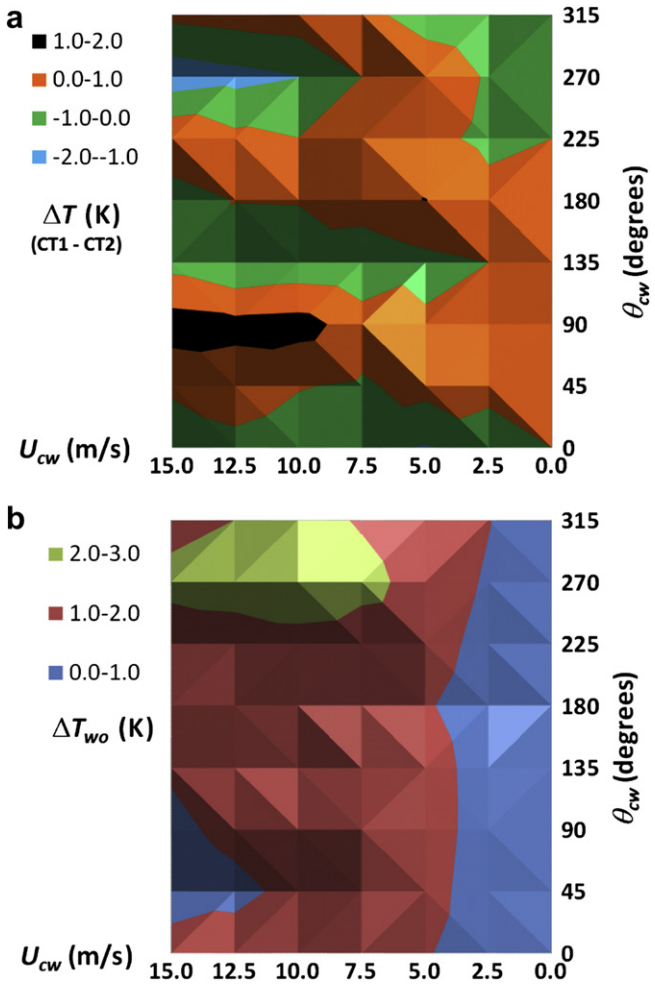

Fig. 7. Coloured contours showing the change in water temperature of the NDWCTs under crosswinds: (a) difference in ΔT (ΔT_{wo}, CT1–ΔT_{wo}, CT2), (b) average water temperature of the two NDWCTs.

velocities have resulted in differences greater than ±0.5 K. Ideally, the two NDWCTs should have the same thermal performance if they both have the same approaching crosswinds conditions. Unfortunately, this situation does not exist in reality and the thermal performance of NDWCTs differs.

For the current PPS arrangement, the assumption of symmetrical conditions with respect to the flow direction is proven invalid. Thus, ΔT_{wo} of the NDWCT is affected by the existence of the other NDWCT and the PPS. Reasons for such differences are found to be dependent on:

- The structure of the approaching crosswinds and whether it is disturbed or undisturbed: The disturbed structure degrades the performance of the NDWCT more than the undisturbed structure.
- The location of the NDWCT in the wake of the other NDWCT: Crosswinds degrades the performance of the NDWCT located in front of another NDWCT more than that located in the wake of another NDWCT.
- The location of the NDWCT in front of/in the wake of the PPS: Crosswinds degrades severely the thermal performance of the NDWCT located in the wake of the PPS. However, crosswinds tend to have less effect on the performance of the NDWCT located in front of the PPS. These results confirmed related results reported earlier by Niemann and Kopper [12].

It is a common practice in power plants to mix the water coming out of the NDWCTs before pumping it back into the condenser. The resulted change in the water temperature ΔT_{wo} after mixing is shown in Fig. 7b. At a crosswinds approaching angle of ($\theta_{cw} = 270^{\circ}$) and speeds of ($U_{cw} > 6$ m/s), the lowest performance has been found ($\Delta T_{wo} > 2.5$ K). However, such a high temperature has occurred for only 13% of the simulated crosswinds velocities. The simulated crosswinds velocities have affected the performance of the NDWCTs by increasing the temperature of the water coming out of them by 1.4 K on average and by 1.0 K for 80% of the simulated case. Regardless of the crosswinds direction, an increase of 1.3 k or more could be predicted at crosswinds speed greater than 4 m/s.

4.2. *Stand-alone* vs. *PPS*

Results from simulating a stand-alone NDWCT have shown that crosswinds speeds of less than 8 m/s could increase the temperature of water coming out of the NDWCT by almost 1.8 K [2]. It also has shown that for speeds greater than 8 m/s, the water temperature decreases due to the airflow structure at outside (inlet of and outlet of) and inside the NDWCT. Effects of the internal airflow on the performance of the NDWCT within PPS are similar to effects on the stand-alone NDWCT. However, Effects of the external airflow structure due to PPS are different from those of the stand-alone NDWCT as have been presented earlier.

The general trend of effects of crosswinds speeds on the NDWCT thermal performance, shown in Fig. 8, is maintained regardless of

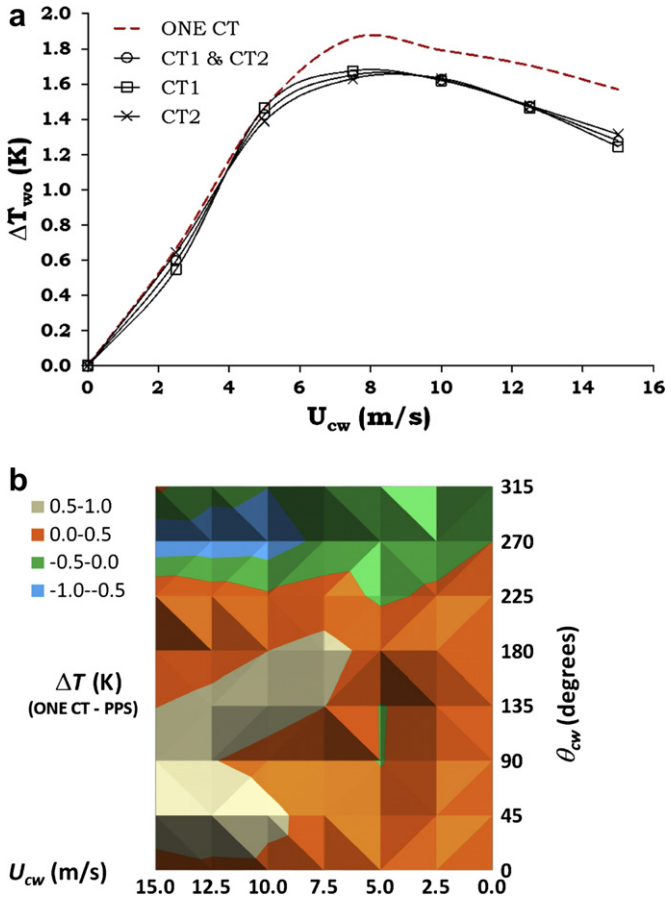

Fig. 8. Differences in water temperature of the NDWCTs: (a) Average ΔT_{wo} across all simulated crosswinds directions at the given speed, (b): of Stand-alone CT – Average ΔT of both NDWCTS within PPS.

the NDWCT being within the PPS or not. The four curves shown in Fig. 8a were the average values of ΔT_{wo} at the given crosswinds speed. For the simulated cases, the change in water temperature (ΔT_{wo}) has increased with the increase of crosswinds speeds ($U_{cw} < 8$ m/s) which is translated into loss of thermal performance and waste of energy. However, high crosswinds speeds ($U_{cw} > 8$ m/s) have shown a positive effect on the NDWCTs performance by reducing the value of ΔT_{wo} as shown by Fig. 8a. Comparing the average effect of crosswinds speeds on the performance of NDWCTs has shown similar qualitative and quantitative results at ($U_{cw} < 6$ m/s). At higher crosswinds speeds, the differences between the performances of the stand-alone CT and the NDWCTs within PPS got larger. These results have shown that the stand-alone CT simulations have underestimated the thermal performance of the NDWCTs at such high speeds and cannot be ignored.

Differences in the average water temperature coming out of the two NDWCTs compared to the stand-alone NDWCT are shown in Fig. 8b. The difference in ΔT_{wo} resulted from the two simulations is less than 1 K for the whole span of crosswinds speeds and could be decreased to 0.7 K for speeds less than 8 m/s. At an approaching angle of ($\theta_{cw} = 270^{\circ}$), the NDWCTs were located in the wake of the PPS which resulted the highest temperature difference ($\Delta T \cong 0.9$ K) at ($U_{cw} > 8$ m/s). Although this is a relatively small difference, it could counts for an annual cost of tens of thousands of dollars.

Results presented here were obtained under the assumption that the NDWCTs are exposed to uniform crosswinds from all direction. Since simulation cost of the full PPS case is much higher than that of a stand-alone case, simulations of a stand-alone NDWCT is a favourable option to understand the physics of the airflow in and around NDWCTs. However, it is inadequate to extrapolate, quantitatively, results obtained from the simulation of a stand-alone NDWCT into NDWCTs within PPS at all θ_{cw}. The location of the NDWCT, with respect to the PPS, and θ_{cw} should be taken into consideration in order to justify the extrapolation of the results as a valid assumption. However, results obtained from a study of a stand-alone NDWCT could be extrapolated, qualitatively, to NDWCTs within PPS simulations.

5. Conclusion

The thermal performance of two adjacent NDWCTs within PPS has been investigated numerically using a general-purpose CFD code (FLUENT). Eight crosswinds directions ($\theta_{cw} = 0^{\circ}, 45^{\circ}, 90^{\circ}, 135^{\circ}, 180^{\circ}, 225^{\circ}, 270^{\circ}$ and 315°) with crosswinds speeds ranging from 0 to 15 m/s were investigated. It has been found that regardless of the crosswinds direction, an increase of 1.3 k or more could be predicted at crosswinds speed greater than 4 m/s. Furthermore, the performance of NDWCTs under crosswinds has been found to be dependent on the three major factors: the structure of the approaching crosswinds and whether it is disturbed or undisturbed, the location of the NDWCT in the wake of the other NDWCT, and the location of the NDWCT in front of/in the wake of the PPS. When comparing results from the stand-alone and from the NDWCTs within PPS simulations, differences in ΔT_{wo} were found to be less than 1 K for the whole span of crosswinds speeds and could be decreased to 0.7 K for speeds less than 8 m/s.

The simulation of stand-alone NDWCT is a very efficient approach in understanding the physics of the airflow in and around the NDWCT. It remains a vital tool to obtain qualitative results that can be implemented into parametric studies before being applied to the full-scale structures.

References

[1] R. Al-Waked, M. Behnia, The performance of natural draft dry cooling towers under crosswind: CFD study, International Journal of Energy Research 28 (2004) 147–161.
[2] R. Al-Waked, M. Behnia, CFD simulation of wet cooling towers, Applied Thermal Engineering 26 (2006) 382–395.
[3] B. Becker, W. Stewart, T. Walter, C. Becker, A numerical model of cooling tower plume recirculation, Mathematical and Computer Modelling 12 (1989) 799–819.
[4] T. Bender, D. Bergstrom, K. Rezkallah, A study on the effects of wind on the air intake flow rate of a cooling tower: part 2. Wind wall study, Journal of Wind Engineering and Industrial Aerodynamics 64 (1996) 61–72.
[5] T. Bender, D. Bergstrom, K. Rezkallah, A study on the effects of wind on the air intake flow rate of a cooling tower: part 3. Numerical study, Journal of Wind Engineering and Industrial Aerodynamics 64 (1996) 73–88.
[6] R. Bornoff, M. Mokhtarzadeh-Dehghan, A numerical study of interacting buoyant cooling-tower plumes, Atmospheric Environment 35 (2001) 589–598.
[7] A. Du Preez, D. Kröger, Effect of wind on performance of a dry-cooling tower, Heat Recovery Systems & CHP 13 (1993) 139–146.
[8] FLUENT user's guide v6.1, FLUENT Incorporated, Lebanon, New Hampshire, 2003.
[9] U. Janicke, L. Janicke, A three-dimensional plume rise model for dry and wet plumes, Atmospheric Environment 35 (2001) 877–890.
[10] S. Majumdar, W. Rodi, Three-dimensional computation of flow past cylindrical structures and model cooling towers, Building and Environment 24 (1989) 3–22.
[11] R. Meroney, Protocol for CFD prediction of cooling-tower drift in an urban environment, Journal of Wind Engineering and Industrial Aerodynamics 96 (2008) 1789–1804.
[12] H. Niemann, H. Kopper, Influence of adjacent buildings on wind effects on cooling towers, Engineering Structures 20 (1998) 874–880.
[13] M. Orlando, Wind-induced interference effects on two adjacent cooling towers, Engineering Structures 23 (2001) 979–992.
[14] H. Panofsky, J. Dutton, Atmospheric Turbulence, John Wiley & Sons, New York, USA, 1984.
[15] W. Ranz, W. Marshall, Evaporation from drops, part I, Chemical Engineering Progress 48 (1952) 141–146.
[16] W. Ranz, W. Marshall, Evaporation from drops, part II, Chemical Engineering Progress 48 (1952) 173–180.
[17] M. Su, G. Tang, S. Fu, Numerical simulation of fluid flow and thermal performance of a dry-cooling tower under cross wind condition, Journal of Wind Engineering and Industrial Aerodynamics 79 (1999) 289–306.
[18] T. Sun, Z. Gu, Interference between wind loading on group of structures, Journal of Wind Engineering and Industrial Aerodynamics 54–55 (1995) 213–225.
[19] T. Sun, Z. Gu, L. Zhou, P. Li, G. Cai, Full-Scale measurement and wind-tunnel testing of wind loading on two neighbouring cooling towers, Journal of Wind Engineering and Industrial Aerodynamics 43 (1992) 2213–2224.